# DIGITAL INTEGRATIVE LQR CONTROL OF A 2DOF HELICOPTER

Fernando dos Santos Barbosa*, Giovanni Gallon Neto*, Bruno Augusto Angélico*

*Laboratório de Controle Aplicado
Dept. Eng. Telecomunicações e Controle
Escola Politécnica da Universidade de São Paulo
São Paulo, SP, Brazil

Emails: barbosa.fs@usp.br, giovanni.neto@usp.br, angelico@lac.usp.br

**Abstract**— A two-degree-of-freedom helicopter is a simple and interesting plant, with nonlinearities and output coupling, allowing the study of several subjects, such as Kalman Filters, sensor fusion, different modeling techniques and usage of classical and modern control. Our main is to develop a digital robust multivariable control for this plant. Therefore, the plants complete model development is shown using Lagrange's method followed by its linearization around an operating point (small angles). Next, a digital LQR controller is projected using anti-windups, since integrators are used at the input of the plant in order to increase the system order and to guarantee null error for the step inputs. Lastly, the controller obtained is simulated and tested on the built helicopter.

**Keywords**— LQR, Digital Control, Helicopter, Integrator

**Resumo**— Um helicóptero com dois graus de liberdade é uma planta simples e interessante, apresentando não-linearidades e acoplamento entre suas saídas, possibilitando o estudo de diferentes assuntos, tais como o uso do Filtro de Kalman, fusão de sensores, emprego de várias técnicas de modelagem e de controle clássico e moderno. O principal objetivo deste artigo é desenvolver um controlador robusto digital multivariável para uma planta deste tipo. Apresenta-se a modelagem completa do sistema com o uso do Método de Lagrange seguido pela sua linearização em torno de um ponto de operação (pequenos ângulos). Em seguida, um controlador LQR digital é projetado fazendo uso de anti-windups, dado que integradores são colocados na entrada da planta para aumentar sua ordem e garantir erro nulo para entrada degrau. Por fim, o controlador obtido é simulado e testado no helicóptero construído.

**Palavras-chave**— LQR, Controle Digital, Helicóptero, Integrador

## 1 Introduction

Aerial vehicles are a trending topic amid engineering students. With the advent of drones and multicopters, they have also gained space in the media and usage in all types of industries, such as cinematography and bridge inspections. Therefore, to study a two-degree-of-freedom (2DOF) helicopter may be a promising start, as it is relatively simpler than 6 DOF vehicles.

Particularly, the helicopter used is a highly non-linear coupled MIMO (Multiple Input, Multiple Output) system (Quanser, 2011) able to rotate only around the pitch and yaw axes. The plant is controlled by two rotors, each composed of a brushless DC motor and a propeller.

Guarnizo et al. (2010) present the complete system modeling and controls a Quanser 2DOF helicopter based on DK-iteration; Camacho et al. (2012) show the construction of a similar helicopter from scratch going through the modeling and tests; Gonzalez et al. (2012) develop a more accurate model also using the Euler-Lagrange equations and designs two control loops, one for each axis, based on observers; Gutierrez et al. (2014) used uncoupled MIMO cross-control and servo tracking control with state observer; Ahmad et al. (2000) and Rahideh and Shaheed (2007) also modeled this plant; Lopez-Martinez et al. (2003) used an $H_\infty$ controller. Lastly, Pérez-D'Arpino et al. (2011) developed a 6 DOF IMU (Inertial Measurement Unit) using Kalman Sensor Fusion.

MIMO systems are easily handled by optimal controllers, allowing the designer to determine feedback gain values using efficient computation tools (Franklin et al., 1997). Linear quadratic regulator is one of the most popular choices for optimal controllers due to its performance index: a quadratic function of the state variable and control inputs. This quadratic performance measure achieves a compromise between minimizing the regulator error and the control effort (Fadali and Visioli, 2013).

This article starts by presenting the modeling of the system using Euler-Lagrange, resulting in both linear and non-linear equations. Then, the digital controller is developed and implemented, followed by its simulation, results and conclusion.

## 2 Mathematical Modeling

The modeling process presented here follows the one shown in Guarnizo et al. (2010) using the Lagrangian method. The system can rotate around two axes, pitch and yaw ($\theta$ and $\psi$), with the following convention:

- Helicopter is horizontal with $\theta = 0$;
- $\dot{\theta}$ is positive when the nose is moving upwards;

- $\dot{\psi}$ is positive when the helicopter rotates CW;
- As the system is fixed, it cannot rotate around the roll axis or move along the axes.

Figure 1 shows a simple free-body diagram of the helicopter model. However, the notation shown in this figure is not the same used in the modeling.

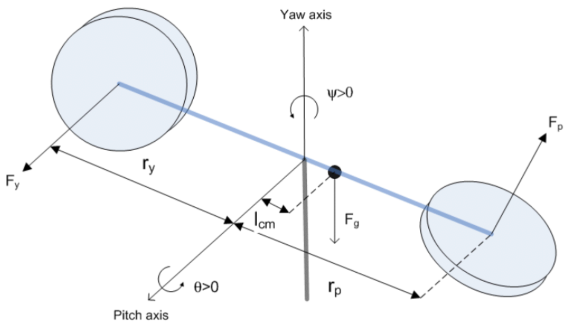


Figure 1: Simple free-body drawing. Adapted from (Quanser, 2011).

Starting the modeling, the total potential energy of the system is given by

$$E_P = m_{heli} g l_{cm} \sin\theta, \tag{1}$$

where $m_{heli}$ is the helicopter total moving mass, $g$ is gravity and $l_{cm}$ the position of the center of mass. The total kinetic energy is

$$\begin{aligned} E_K = {} & \frac{1}{2} J_{eq\_p} \dot{\theta}^2 + \frac{1}{2} J_{eq\_y} \dot{\psi}^2 + \frac{1}{2} m_{heli} \\ & \Big[ \Big( -\sin(\psi)\dot{\psi}\cos(\theta) l_{cm} - \cos(\psi)\sin(\theta)\dot{\theta} l_{cm} \Big)^2 \\ & + \Big( -\cos(\psi)\dot{\psi}\cos(\theta) l_{cm} + \sin(\psi)\sin(\theta)\dot{\theta} l_{cm} \Big)^2 \\ & + \cos(\theta)^2 \dot{\theta}^2 l_{cm}^2 \Big]. \end{aligned} \tag{2}$$

$J_{eq\_p}$ and $J_{eq\_y}$ are the helicopter moments of inertia around pitch and yaw. As aforementioned, the system is controlled by two BLDC electric motors, each generating torque to both axes. For example, the pitch motor directly controls the pitch angle using the force generated by its propeller, creating torque in the yaw as an effect of air resistance. Then, the torques for each axis can be written as:

$$\tau_p = K_{pp} V_{m\_p} + K_{py} V_{m\_y} \tag{3}$$

$$\tau_y = K_{yy} V_{m\_y} + K_{yp} V_{m\_p} \tag{4}$$

wherein $K_{pp}$ is the pitch motor torque constant on the pitch axis, $K_{py}$ is the yaw motor torque constant on the pitch axis, $K_{yp}$ is the pitch motor torque constant on the yaw axis, $K_{yy}$ is the yaw motor torque constant on the yaw axis, $V_{m\_p}$ and $V_{m\_y}$ are the pitch and yaw motors signal percentage. The generalized forces vector is given by

$$\begin{aligned} \mathbf{Q} = [Q_1, Q_2] = \Big[ & K_{pp} V_{m\_p} + K_{py} V_{m\_y} - B_p \dot{\theta}, \\ & K_{yy} V_{m\_y} + K_{yp} V_{m\_p} - B_y \dot{\psi} \Big] \end{aligned} \tag{5}$$

with $B_p$ and $B_y$ being the air resistance acting on the pitch and yaw axes, respectively. Lagrange's equation is written as:

$$\begin{aligned} \frac{\partial}{\partial t} \frac{\partial L}{\partial \dot{q_1}} - \frac{\partial}{\partial q_1} L &= Q_1 \\ \frac{\partial}{\partial t} \frac{\partial L}{\partial \dot{q_2}} - \frac{\partial}{\partial q_2} L &= Q_2, \end{aligned} \tag{6}$$

where $q_1$ and $q_2$ are the generalized coordinates $\theta$ and $\psi$, respectively, and $L$ is the Lagrangian of the system, defined by the difference between the total kinetic energy and the total potential energy of the system.

Solving the Euler-Lagrange's equation results in a non-linear equation of motion:

$$\ddot{\theta} = \frac{K_{pp} V_{m\_p} + K_{py} V_{m\_y} - \Big( B_p \dot{\theta} + \alpha + \beta \Big)}{J_{eq\_p} + m_{heli} l_{cm}^2} \tag{7}$$

$$\alpha = m_{heli} l_{cm}^2 \dot{\psi}^2 \sin(\theta)\cos(\theta) \tag{8}$$

$$\beta = m_{heli} g \cos(\theta) l_{cm} \tag{9}$$

$$\ddot{\psi} = \frac{K_{yp} V_{m\_p} + K_{yy} V_{m\_y} + \gamma - B_y \dot{\psi}}{J_{eq\_y} + m_{heli} \cos(\theta)^2 l_{cm}^2} \tag{10}$$

$$\gamma = 2 m_{heli} l_{cm}^2 \sin(\theta)\cos(\theta)\dot{\psi}\dot{\theta} \tag{11}$$

By linearizing the system for small angles, as this is the operating point, the equations of motion are defined by

$$\ddot{\theta} = \frac{K_{pp} V_{m\_p} + K_{py} V_{m\_y} - B_p \dot{\theta} - m_{heli} g l_{cm}}{J_{eq\_p} + m_{heli} l_{cm}^2} \tag{12}$$

$$\ddot{\psi} = \frac{K_{yp} V_{m\_p} + K_{yy} V_{m\_y} - B_y \dot{\psi}}{J_{eq\_y} + m_{heli} l_{cm}^2}. \tag{13}$$

A state-space system is written based on these equations, resulting in:

$$\begin{aligned} \dot{\mathbf{x}}(t) &= \mathbf{A}\mathbf{x}(t) + \mathbf{B}\mathbf{u}(t) \\ \mathbf{y}(t) &= \mathbf{C}\mathbf{x}(t) \end{aligned} \tag{14}$$

where $\mathbf{x}(t)$ corresponds to the states of the system and $\mathbf{u}(t)$ to the percentage inputs of the motor, defined by:

$$\mathbf{x}(t) = \begin{bmatrix} \theta(t) & \psi(t) & \dot{\theta}(t) & \dot{\psi}(t) \end{bmatrix}^T \tag{15}$$

$$\mathbf{u}(t) = \begin{bmatrix} V_{m\_p}(t) & V_{m\_p}(t) \end{bmatrix}^T. \tag{16}$$

ISSN 2525-8311 

The matrices $A$, $B$ and $C$ are then written as

$$\mathbf{A} = \begin{bmatrix} 0 & 0 & 1 & 0 \\ 0 & 0 & 0 & 1 \\ 0 & 0 & \frac{-B_p}{J_{eq\_p}+m_{heli}l_{cm}^2} & 0 \\ 0 & 0 & 0 & \frac{-B_y}{J_{eq\_y}+m_{heli}l_{cm}^2} \end{bmatrix}$$

$$\mathbf{B} = \begin{bmatrix} 0 & 0 \\ 0 & 0 \\ \frac{K_{pp}}{J_{eq\_p}+m_{heli}l_{cm}^2} & \frac{K_{py}}{J_{eq\_p}+m_{heli}l_{cm}^2} \\ \frac{K_{yp}}{J_{eq\_y}+m_{heli}l_{cm}^2} & \frac{K_{yy}}{J_{eq\_y}+m_{heli}l_{cm}^2} \end{bmatrix}$$

$$\mathbf{C} = \begin{bmatrix} 1 & 0 & 0 & 0 \\ 0 & 1 & 0 & 0 \end{bmatrix}.$$

## 3 The Helicopter

For constructing the model, presented in Figure 2, two brushless DC motors were used as actuators to control the yaw and pitch angles; two encoders were used for measuring these angles. As the simple and cheap Electronic Speed Controllers (ESCs), responsible controlling brushless motors, can only rotate their motor in one direction, choosing motors with enough torque to rotate the model is important. A development platform based on ARM architecture was used to interface sensors, ESCs and processing.

In order to identify the rotors characteristics, a platform was used to measure a rotor thrust and torque. Their relation to the input signal was approximated by polynomial equations and linearized to get the parameters of equations (3) and (4).

The rest of the parameters were obtained by simple system identification, presented in Table 1. It is worth explaining the $K_{pp}$, $K_{yy}$, $K_{py}$ and $K_{yp}$ signals: they are positive if they act to positively increase their respective angle of effect, e.g., $K_{pp}$ brings the nose upward (positive pitch) while $K_{yy}$ rotates the helicopter CCW (negative YAW).

Table 1: Helicopter Parameters

| Parameter | Value | Unit |
|---|---|---|
| $m_{heli}$ | 1.317 | $kg$ |
| $l_{cm}$ | 0.038 | $m$ |
| $K_{pp}$ | 0.0180 | $N.m/\%$ |
| $K_{yy}$ | $-0.0033$ | $N.m/\%$ |
| $K_{py}$ | $-6.35 \times 10^{-4}$ | $N.m/\%$ |
| $K_{yp}$ | $10.76 \times 10^{-4}$ | $N.m/\%$ |
| $B_p$ | 0.1 | $N/\%$ |
| $B_y$ | 0.1 | $N/\%$ |
| $J_{eq\_p}$ | 0.384 | $kg.m^2$ |
| $J_{eq\_q}$ | 0.0432 | $kg.m^2$ |

## 4 Digital Controller

Two paths may be taken to use a digital controller: to develop the entire project in continuous time and then discretize the final controller; or to start by plant discretization and then project the controller already in discrete time (Castrucci et al., 2011). Since the second was chosen, a discrete-time system equivalent to (14) is written as:

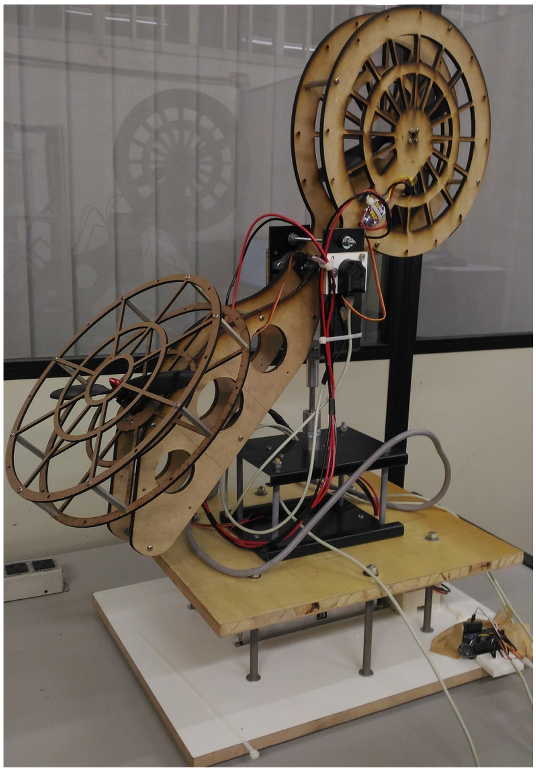

Figure 2: 2DOF Helicopter built.

$$\begin{aligned} \mathbf{x}[n+1] &= \mathbf{\Phi}\mathbf{x}[n] + \mathbf{\Gamma}\mathbf{u}[n] \\ \mathbf{y}[n] &= \mathbf{C}\mathbf{x}[n]. \end{aligned} \quad (17)$$

Matrices $\mathbf{\Phi}$ and $\mathbf{\Gamma}$ are obtained from the continuous-time $\mathbf{A}$ and $\mathbf{B}$ taking the 100Hz sampling time into account. The resulting matrices are:

$$\mathbf{\Phi} = \begin{bmatrix} 1 & 0 & 0.0100 & 0 \\ 0 & 1 & 0 & 0.0099 \\ 0 & 0 & 0.9974 & 0 \\ 0 & 0 & 0 & 0.9781 \end{bmatrix}, \quad (18)$$

$$\mathbf{\Gamma} = \begin{bmatrix} 2.33 \cdot 10^{-6} & -8.22 \cdot 10^{-8} \\ 1.18 \cdot 10^{-6} & -3.65 \cdot 10^{-6} \\ 4.66 \cdot 10^{-4} & -1.64 \cdot 10^{-5} \\ 2.36 \cdot 10^{-4} & -7.27 \cdot 10^{-4} \end{bmatrix}. \quad (19)$$

A state feedback controller $\mathbf{u}[n] = -\mathbf{K}\mathbf{x}[n]$ that minimizes the cost function

$$J = \frac{1}{2}\sum_{n=0}^{\infty}\left(\mathbf{x}^T[n]\mathbf{Q}\mathbf{x}[n] + \mathbf{u}^T[n]\mathbf{R}\mathbf{u}[n]\right) \quad (20)$$

is the discrete version of the Linear Quadratic Regulator (LQR) for systems as (17). Each plant channel receives an integrator to guarantee zero steady-state error for the step inputs, as shown in Figure 3.

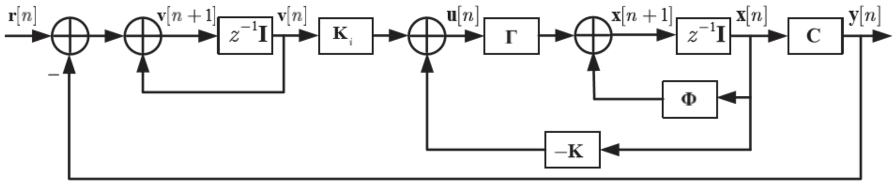

Figure 3: Integrator insertion.

The integrator state equation may be written as follows:

$$\begin{aligned}\mathbf{v}[n+1] &= \mathbf{v}[n] + \mathbf{r}[n] - \mathbf{y}[n] \\ &= \mathbf{v}[n] + \mathbf{r}[n] - \mathbf{C}\mathbf{x}[n] \end{aligned} \tag{21}$$

and the closed-loop equation is (Fadali and Visioli, 2013)

$$\mathbf{x}[n+1] = (\mathbf{\Phi} - \mathbf{\Gamma}\mathbf{K})\,\mathbf{x}[n] + \mathbf{\Gamma}\mathbf{K_i}\mathbf{v}[n]. \tag{22}$$

Therefore, the complete augmented system has the following equation:

$$\begin{bmatrix}\mathbf{x}[n+1]\\ \mathbf{v}[n+1]\end{bmatrix} = \begin{bmatrix}\mathbf{\Phi}-\mathbf{\Gamma}\mathbf{K} & \mathbf{\Gamma}\mathbf{K_i}\\ -\mathbf{C} & \mathbf{I}_{2,2}\end{bmatrix}\cdot \underbrace{\begin{bmatrix}\mathbf{x}[n]\\ \mathbf{v}[n]\end{bmatrix}}_{\hat{\mathbf{x}}[n]} + \begin{bmatrix}\mathbf{0}_{4,2}\\ \mathbf{I}_{2,2}\end{bmatrix}\cdot\mathbf{r}[n], \tag{23}$$

wherein $\hat{\mathbf{x}}[n]$ is the new augmented states vector and the state matrix expands as

$$\underbrace{\begin{bmatrix}\mathbf{\Phi} & \mathbf{0}_{4,2}\\ -\mathbf{C} & \mathbf{I}_{2,2}\end{bmatrix}}_{\hat{\mathbf{\Phi}}} - \underbrace{\begin{bmatrix}\mathbf{\Gamma}\\ \mathbf{0}_{2,2}\end{bmatrix}}_{\hat{\mathbf{\Gamma}}}\cdot\underbrace{\begin{bmatrix}\mathbf{K} & -\mathbf{K_i}\end{bmatrix}}_{\hat{\mathbf{K}}} \tag{24}$$

and each matrix stands for new augmented $\hat{\mathbf{\Phi}}$, $\hat{\mathbf{\Gamma}}$ and $\hat{\mathbf{K}}$.

As matrices **Q** and **R** are weakly connected to performance specifications, the *pincer* procedure (Franklin et al., 1997) creates a new degree of freedom for the controller to keep the closed-loop poles inside a $^1/_\alpha$ radius circle, with $\alpha > 1$. Assuming the following modified cost function

$$\begin{aligned}J = \frac{1}{2}\sum_{n=0}^{\infty}\Big[&(\alpha^n\hat{\mathbf{x}}[n])^T\,\mathbf{Q}\,(\alpha^n\hat{\mathbf{x}}[n]) \\ &+ (\alpha^n\mathbf{u}[n])^T\,\mathbf{R}\,(\alpha^n\mathbf{u}[n])\Big],\end{aligned} \tag{25}$$

then

$$\begin{aligned}\alpha^{n+1}\hat{\mathbf{x}}[n+1] &= \alpha^{n+1}\left(\hat{\mathbf{\Phi}}\hat{\mathbf{x}}[n] + \hat{\mathbf{\Gamma}}\mathbf{u}[n]\right) \\ &= \alpha\hat{\mathbf{\Phi}}\,(\alpha^n\hat{\mathbf{x}}[n]) + \alpha\hat{\mathbf{\Gamma}}\,(\alpha^n\mathbf{u}[n])\,,\end{aligned} \tag{26}$$

and the optimal control problem may be formulated as $\alpha^n\mathbf{u}[n] = -\hat{\mathbf{K}}\,(\alpha^n\hat{\mathbf{x}}[n])$, i.e., $\mathbf{u}[n] = -\hat{\mathbf{K}}\hat{\mathbf{x}}[n]$. Finally, $\alpha$ is defined as $100^{T_s/t_s}$, with $T_s$ the sampling time and $t_s$ the settling time chosen for a 1% criteria (Franklin et al., 2001).

Lastly, to determine the **Q** and **R** matrices, Bryson's rule (Franklin et al., 2001) suggests choosing diagonal matrices such that:

$$\begin{aligned}Q_{ii} &= \frac{1}{(\max x_i)^2},\\ R_{jj} &= \frac{1}{(\max u_j)^2},\end{aligned} \tag{27}$$

in which $i$ is the state and $j$ the control input.

By using $t_s = 10s$ and the following **Q** and **R** matrices

$$\mathbf{Q} = \begin{bmatrix}1&0&0&0&0&0\\0&1&0&0&0&0\\0&0&5&0&0&0\\0&0&0&5&0&0\\0&0&0&0&0&0\\0&0&0&0&0&0\end{bmatrix} \tag{28}$$

$$\mathbf{R} = \begin{bmatrix}90^{-2} & 0\\ 0 & 50^{-2}\end{bmatrix} \tag{29}$$

the resulting gain matrix was:

$$\hat{\mathbf{K}} = \left[\begin{array}{llll}418.8146 & 71.8968 & 233.6604 & \ldots\\ 57.3546 & -243.4466 & 36.9813 & \ldots\end{array}\right.$$
$$\left.\begin{array}{llll}\ldots & 35.8345 & -1.9874 & -0.3618\\ \ldots & -110.8521 & -0.2527 & 1.1461\end{array}\right]. \tag{30}$$

## 5 Simulation and Results

The first step was simulating the complete system with Simulink. The control commands were manually programmed, as would be done in a microcontroller; here is where the anti-windup part was considered. Not considering the anti-windup may seem good initially but its usage guarantees that the integral error will not grow beyond the motors limits, causing a slow response after the system gets back to the normal conditions of operation. Motors saturations and dead-zones were also included.

The simulation procedure was as follows:

- During the first seconds, wait for the system to stabilize at $\theta = 0$ and $\psi = 0$;
- at 20s, give a step reference of 0.35rad for the pitch and at 35s a step reference of −0.35rad for the yaw;
- at 50s, give a new reference to take the pitch back to zero and do the same to the yaw at 65s.

Figure 4 shows all the four states and their response to the simulation procedure, proving the stabilization capability of the digital optimal controller developed. The control effort is shown in Figure 5, in which is interesting to notice that the pitch control effort is maximum when the helicopter is horizontal.

The next step was uploading the controller to the development board and controlling the real helicopter. The same test procedure presented for the simulation was used.

Figure 6 presents the real system response, in which it is possible to verify the stabilization capability of the controller developed. Figure 7 shows the respective motor percentage. The main differences from the simulated system may be caused by poor system identification as well as by the power cable position, causing unmodeled dynamics.

## 6 Conclusion

It was presented the complete development of the digital integrative LQR controller using Bryson's rule and pincer procedure. This optimal controller was capable of not only stabilizing the helicopter but also taking it to points far from the operating one chosen for linearization.

In normal conditions of operation, there is no need to implement an anti-windup code, since both motors are far from saturation. However, if considering a system with the possibility of external forces acting on it, the anti-windup is advised.

Different choices of $Q$ and $R$ matrices and $\alpha$ would force the system to react in different manners. Changing them allows the system to respond faster or slower, remembering to always be cautious of the control effort.

Future works consist in performing better system identification, implementing filters and testing different controllers.

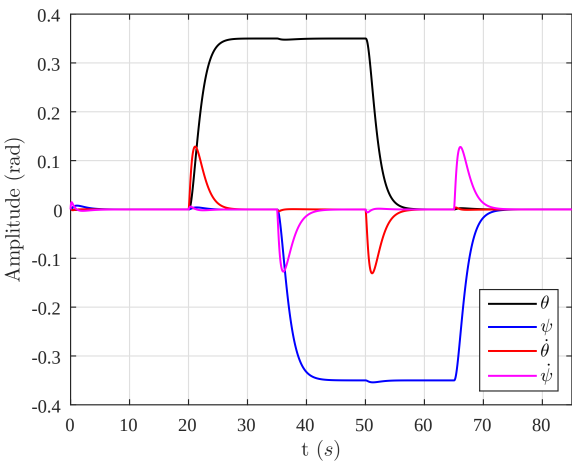


Figure 4: System states for non-linear model simulation. $\theta$ and $\psi$ are in rad, $\dot{\theta}$ and $\dot{\psi}$ in rad/s.

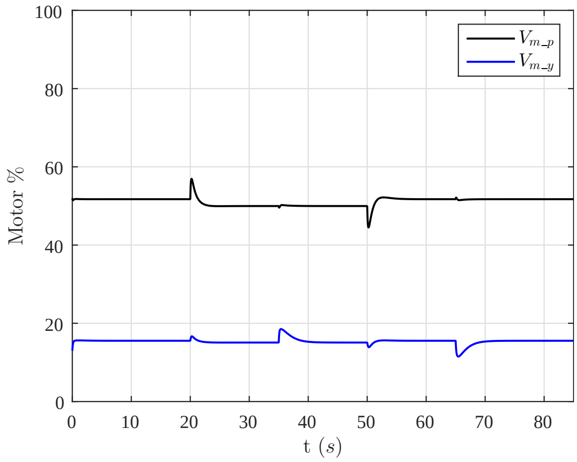


Figure 5: Motors percentage for non-linear model simulation.

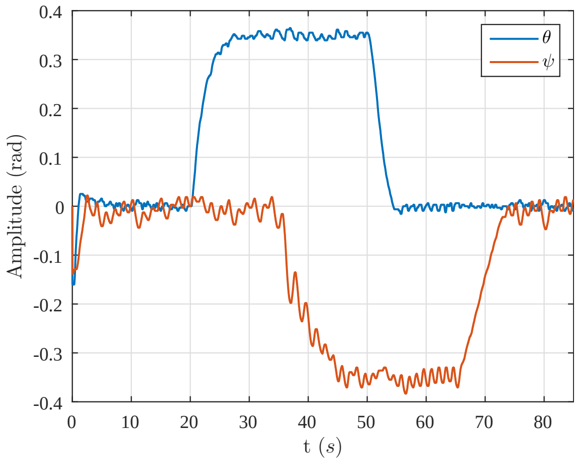


Figure 6: Results from the controller applied to the built helicopter.

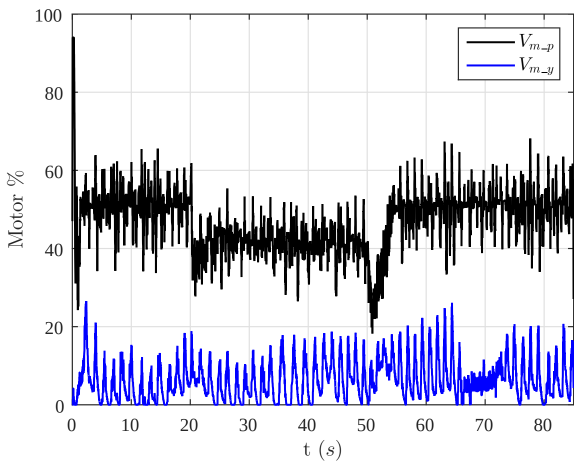


Figure 7: Motors percentage used to control the built helicopter.

**Acknowledgment**

The authors would like to thank the Programa de Excelência Acadêmica (Proex) from the Coordination for the Improvement of Higher Education Personnel (CAPES) for grant 0212083 and the National Counsel of Technological and Scientific Development (CNPq) for grant 151881/2015-4. We also thank Kennedy X. B. Peixoto for his incredible work and help with building the helicopter and Freescale for donating the FRDM-K64F development platforms.

## References

Ahmad, S., Chipperfield, A. and Tokhi, M. (2000). Dynamic modeling and optimal control of a twin rotor mimo system, *National Aerospace and Electronics Conference, 2000. NAECON 2000. Proceedings of the IEEE 2000*, pp. 391–398.

Camacho, K., Burgos, J. and Combita, L. (2012). Construction and modeling of a two-degree-of-freedom helicopter, *Robotics Symposium and Latin American Robotics Symposium (SBR-LARS), 2012 Brazilian*, pp. 150–155.

Castrucci, P., Bittar, A. and Moura Sales, R. (2011). *Controle Automático*, LTC.

Fadali, M. and Visioli, A. (2013). *Digital Control Engineering - Analysis and Design*, 2nd edn, Elsevier.

Franklin, G. F., Powell, D. J. and Emami-Naeini, A. (2001). *Feedback Control of Dynamic Systems*, 4th edn, Prentice Hall PTR, Upper Saddle River, NJ, USA.

Franklin, G. F., Workman, M. L. and Powell, D. (1997). *Digital Control of Dynamic Systems*, 3rd edn, Addison-Wesley Longman Publishing Co., Inc., Boston, MA, USA.

Gonzalez, E., Rivera, D. and Gomez, E. (2012). Model and observer-based controller design for a quanser helicopter with two dof, *Electronics, Robotics and Automotive Mechanics Conference (CERMA), 2012 IEEE Ninth*, pp. 267–271.

Guarnizo, M., Trujillo, R. and Guacaneme, M. (2010). Modeling and control of a two dof helicopter using a robust control design based on dk iteration, *IECON 2010 - 36th Annual Conference on IEEE Industrial Electronics Society*, pp. 162–167.

Gutierrez, J., Duarte, E. and Arcos, J. (2014). Control systems for a helicopter with two degrees of freedom, *III International Congress of Engineering Mechatronics and Automation (CIIMA)*, pp. 1–6.

Lopez-Martinez, M., Ortega, M. and Rubio, F. (2003). An h infin; controller for a double rotor system, *Emerging Technologies and Factory Automation, 2003. Proceedings. ETFA '03. IEEE Conference*, Vol. 1, pp. 253–259.

Pérez-D'Arpino, C., Vigouroux, D., Medina-Melendez, W., Fermin, L., Torrealba, R., Grieco, J. and Fernandez-Lopez, G. (2011). Development of a low cost inertial measurement unit for uav applications with kalman filter based attitude determination, *Technologies for Practical Robot Applications (TePRA), 2011 IEEE Conference on*, pp. 178–183.

Quanser (2011). *Quanser 2-DOF Helicopter - Laboratory Manual*, 2.0 edn, Quanser Inc.

Rahideh, A. and Shaheed, M. H. (2007). Mathematical dynamic modelling of a twin-rotor multiple input-multiple output system, *Proceedings of the Institution of Mechanical Engineers, Part I: Journal of Systems and Control Engineering* **221**(1): 89–101.